Structure of Turbulent Velocity and Scalar Fields at Large Wavenumbers

Yih-Ho Pao

Citation: The Physics of Fluids **8**, 1063 (1965); doi: 10.1063/1.1761356
View online: https://doi.org/10.1063/1.1761356
View Table of Contents: https://aip.scitation.org/toc/pfl/8/6
Published by the American Institute of Physics

Structure of Turbulent Velocity and Scalar Fields at Large Wavenumbers

YIH-HO PAO
Boeing Scientific Research Laboratories, Seattle, Washington
(Received 14 October 1964; final manuscript received 15 February 1965)

For incompressible turbulent flow with large Reynolds and Péclet numbers, mechanisms for the spectral transfer of kinetic energy, heat, and mass at large wavenumbers are proposed. Based on these mechanisms, turbulent energy, temperature, and the concentration spectrum functions are deduced for the entire universal equilibrium range of wavenumbers. The resulting one-dimensional energy, temperature, and concentration spectra are compared with measurements.

I. INTRODUCTION

"BIG whirls have little whirls, that feed on their velocity; and little whirls have lesser whirls, and so on to viscosity." In this rhyme, by L. F. Richardson, lies the original idea of turbulent energy transfer. Based on Richardson's physical idea that the turbulent flow contains eddies of various sizes, and the energy is transferred from larger eddies to smaller eddies until it is drained out by viscous dissipation, Kolmogorov[1] further postulated (Kolmogorov's first hypothesis) that for large Reynolds numbers, the small-scale components (small eddies) of turbulence are statistically steady, isotropic, and independent of the detailed structure of the large-scale components (large eddies) of turbulence. The motion associated with the small-scale components is uniquely determined by two parameters: one is the kinematic viscosity ν, and the other is ϵ, which is the rate that the turbulent energy per unit mass is fed to the small-scale components from the large-scale components. Consequently, for small separation $\mathbf{r}$, the turbulent velocity difference[1] (the velocity structure function) is,

$$\overline{|\mathbf{u}(\mathbf{x}+\mathbf{r}, t)-\mathbf{u}(\mathbf{x}, t)|^2} = (\epsilon r)^{\frac{2}{3}} B(r/\eta), \quad r \ll L, \qquad (1.1)$$

where $\eta = (\nu^3/\epsilon)^{\frac{1}{4}}$ is the Kolmogorov length scale, which is a characteristic length for the small eddies; $r = |\mathbf{r}|$; L is the characteristic length for the energy-containing eddies. In the wavenumber space, the energy spectrum functions at large wavenumbers (small scales) are universal, and dimensional analysis gives[2,3]

$$E(k, t) = \epsilon^{2/3} k^{-5/3} A(k/k_K), \qquad k_0 \ll k, \qquad (1.2)$$

where k is the wavenumber; $k_0 = (1/L)$; $k_K = (1/\eta)$ is the Kolmogorov wavenumber. $k \gg k_0$ is called the universal equilibrium range of wavenumbers. $A(k/k_K)$ and $B(r/\eta)$ are dimensionless functions of universal form, which are not determinant from the above hypothesis. When the Reynolds number is large enough for the energy-containing eddies to be much larger than the viscous dissipation eddies ($L \ggg \eta$), Kolmogorov[1] further postulated (Kolmogorov's second hypothesis) that there exists a subrange in which negligible dissipation occurs and the transfer of energy by inertia forces is the dominant process. This range is called the inertial subrange, $\eta \ll r \ll L$. The motion associated with the inertial subrange is therefore determined uniquely by ϵ. Dimensional reasoning gives[1]

$$\overline{|\mathbf{u}(\mathbf{x}+\mathbf{r}, t)-\mathbf{u}(\mathbf{x}, t)|^2} = \beta \epsilon^{\frac{2}{3}} r^{\frac{2}{3}}, \quad \eta \ll r \ll L, \qquad (1.3)$$

where β is a constant. Accordingly, the energy spectrum function for the inertial subrange is[2,3]

$$E(k, t) = \alpha \epsilon^{2/3} k^{-5/3}, \qquad k_0 \ll k \ll k_K, \qquad (1.4)$$

where α is a constant. Therefore, in the inertial subrange the universal functions $A(k/k_K)$ and $B(r/\eta)$ reduce to constants α and β, respectively. The idea that the statistical behavior of small-scale components are universal was partly anticipated by Obukhov[4] and suggested independently by Onsager[5,6] and von Weizsäcker.[7]

These hypotheses and their consequences have received considerable experimental support to warrant their validity. The hypothesis that the small-scale components are isotropic (concept of local isotropy) and their behaviors universal has received support from many measurements in various turbu-

[1] A. N. Kolmogorov, C. R. Acad. Sci. USSR **30**, 301 (1941).

[2] G. K. Batchelor, *The Theory of Homogeneous Turbulence* (Cambridge University Press, Cambridge, 1953), Chaps. 5 and 6.

[3] G. K. Batchelor, Proc. Cambridge Phil. Soc. **43**, 533 (1947).

[4] A. M. Obukhov, C. R. Acad. Sci. USSR **32**, 19 (1941); Izv. Akad. Nauk. SSSR, Ser Geogr. i. Geofiz. **5**, 453 (1941), (translation issued by Ministry of Supply, United Kingdom, as P21109T).

[5] L. Onsager, Phys. Rev. **68**, 286 (1945).

[6] L. Onsager, Nuovo Cimento Suppl. **6**, 279 (1949).

[7] C. F. von Weizsäcker, Z. Physik **124**, 614 (1948).

lent flows with different Reynolds numbers.[8-25] Furthermore, the recent measurements of energy spectra in turbulent flow with very large Reynolds numbers—by Gurvich,[19] in a wind over land; by Pond *et al.*,[25] in a wind over waves; by Grant *et al.*,[21,22] in a tidal stream; and by Gibson,[23] in a round jet—further show that the spectra are proportional to $k^{-5/3}$ in the inertial subrange, which supports (1.4).

Kolmogorov's hypotheses enable us to predict the behavior of small-scale components in the inertial subrange explicitly, but shed no light on the forms of the universal functions $A(k/k_K)$ and $B(r/\eta)$ at larger wavenumbers at which the viscous dissipation is important—dissipation subrange, $k \geq k_K$. Furthermore, they provide no information as to how the energy is transferred at large wavenumbers. To understand the detailed structure of energy distribution in the universal range, energy transfer theories, each based on a different physical mechanism which predicts the energy spectra in the universal range ($k \gg k_0$), have been proposed by Obukhov,[4] Kovasznay,[26] and Heisenberg.[27] The energy spectra predicted by these theories all reduce to $k^{-5/3}$ form in the inertial subrange and are in moderate agreement with observations for $k < k_K$, as compared recently by Ellison.[28] However, it is unlikely that these theories—and other similar ones[28-30]—are applicable at larger wavenumbers $k \geq k_K$. The reasons will be discussed in the following paragraph.

Obukhov,[4] using the analogy with the expression for turbulent energy production in a shear flow, obtained an energy spectrum function; but it increases with wavenumber for very large wavenumbers, which is physically impossible. Ellison[28] modified Obukhov's model and obtained a monotonically decreasing energy spectrum function, but it still does not agree with measurements at very large wavenumber. Kovasznay[26] has assumed that the rate of energy transfer across a wavenumber depends only on the energy spectrum function and wavenumber. He obtained a power-law spectrum which demands a cutoff at large wavenumber. Heisenberg's[27] transfer theory, which has received by far the most attention among the three, regards the action of small eddies as equivalent to an eddy viscosity, which leads to an energy spectrum function of k^{-7} for very large wavenumbers. The objection to a power-law spectrum, as pointed out by Stewart and Townsend,[12] is that sufficiently high-order moments of the spectrum become infinite; this infers the nonexistence of higher order velocity derivatives. Furthermore, comparisons of experimental measurements with Heisenberg's spectra,[28,31,32] Kovasznay's spectra[28,33] and modified Obukhov's spectra[28] show that the predicted spectra do not agree with measurements in the dissipation subrange ($k \geq k_K$).

By assuming that the small-scale variations of vorticity occur mainly as isolated sheets or lines of concentrated vorticity, and that they are under uniform straining motion, Townsend[13] obtained an energy spectrum function at very large wavenumbers, $k \geq k_K$. The actual form of the spectrum function is dependent on the manner the vortices are stretched, which is not precisely known. Saffman[34] modified Townsend's uniform straining model without using the concept of isolated vortex sheets or lines. In addition to the indeterminancy of the energy spectrum form, the objection to these models is that the vorticity and the rate of strain are related quantities; it is rather difficult to visualize the coexistence of the random vorticity field and the uniform straining field.

An approximation scheme, based on a sequence of modified perturbation expansions, has been proposed

[8] A. A. Townsend, Proc. Cambridge Phil. Soc. **44**, 560 (1948).
[9] S. Corrsin, J. Aeron. Sci. **16**, 757 (1949).
[10] S. Corrsin, and M. S. Uberoi, NACA Report 1040 (1951).
[11] G. K. Batchelor and A. A. Townsend, Proc. Roy. Soc. (London) **A199**, 238 (1949).
[12] R. W. Stewart and A. A. Townsend, Phil. Trans. Roy. Soc. London **A243**, 359 (1951).
[13] A. A. Townsend, Proc. Roy. Soc. (London) **A208**, 534 (1951).
[14] H. W. Liepmann, J. Laufer, and K. Liepmann, NACA Technical Note 2473 (1951).
[15] J. Laufer, NACA Report 1053 (1951).
[16] Laufer, J., NACA Report 1174 (1954).
[17] P. S. Klebanoff, NACA Report 1247 (1955).
[18] R. Betchov, J. Fluid Mech. **3**, 205 (1957).
[19] A. S. Gurvich, Izv. Akad. Nauk. SSSR, Geofiz. **7** (1960); Bull. Acad. Sci. USSR, Geophys. Ser. No. 7, 1042 (1960).
[20] A. L. Kistler, and T. Vrebalovich, Bull. Am. Phys. Soc. **6**, 207 (1961).
[21] H. L. Grant, R. W. Stewart, and A. Moilliet, J. Fluid Mech. **12**, 241 (1962).
[22] H. L. Grant, and A. Moilliet, J. Fluid Mech. **12**, 237 (1962).
[23] M. M. Gibson, J. Fluid Mech. **15**, 161 (1963).
[24] C. H. Gibson, and W. H. Schwarz, J. Fluid Mech. **16**, 365 (1963).
[25] S. Pond, R. W. Stewart, and R. W. Burling, J. Atmospheric Sci. **20**, 319 (1963).
[26] L. S. G. Kovasznay, J. Aeron. Sci. **15**, 745 (1948).
[27] W. Heisenberg, Z. Physik **124**, 628 (1948) [English transl.: NACA TM 1431 (1958)].
[28] T. H. Ellison, in *Colloques International du Centre National de la Recherche Scientifique* (Editions du Centre National de la Recherche Scientifique, Paris, 1962), No. 108, p. 113.
[29] T. von Kármán, Proc. Natl. Acad. U.S. **34**, 530 (1948).
[30] S. Goldstein, Proc. Cambridge Phil. Soc. **47**, 554 (1951).
[31] S. Chandrasekhar, Proc. Roy. Soc. (London) **A200**, 20 (1949).
[32] I. Proudman, Proc. Cambridge Phil. Soc. **47**, 158 (1951).
[33] W. H. Reid, Phys. Fluids **3**, 72 (1960).
[34] P. G. Saffman, J. Fluid Mech. **16**, 545 (1963).

by Kraichnan.[35] The lowest order nontrivial approximation is termed the direct-interaction approximation. At large enough Reynolds number for an inertial subrange to occur, the direct interaction approximation overestimates spectrum levels at large wavenumbers, leading to a $k^{-3/2}$ inertial subrange law instead of the $k^{-5/3}$ law of Kolmogorov.

Based on an analogy with radiative transfer in an inhomogeneous medium, Kraichnan and Spiegel[36] proposed a model for energy transfer at wavenumbers below, as well as above, the energy containing range in isotropic turbulence. In this model, the triad interactions of the Fourier modes is approximated by interaction between pairs of modes.

Recently, Kraichnan[37] has further proposed a closure approximation termed Lagrangian-history direct-interaction approximation; preliminary spectrum computation seems to agree with measurements.

Edwards[38] recently has proposed an approximation scheme based on a Fokker–Planck type approximation. No detailed numerical computation has yet been made of this approximation.

For the corresponding problems of turbulent mixing of scalar quantities such as concentration, temperature, etc., Obukhov[39] and Corrsin[40] extended Kolmogorov's second hypothesis to investigate the small scale structure of the fluctuating scalar field, $\theta(\mathbf{x}, t)$. When the Reynolds number and the Péclet number are sufficiently large for the θ-containing eddies (of scale L_θ) to be much larger than the diffusive eddies (of scale η_θ), then there exists a convective subrange in which negligible molecular diffusion occurs and transfer of concentration content by turbulent convection is the dominant process. In this subrange, the behavior of small scale θ components are uniquely determined by ϵ, χ. χ is the rate at which the scalar quantity is fed into the small scale components. Dimensional reasoning gives[39,40] the θ-structure function as

$$\overline{(\theta' - \theta)^2} = q\chi\epsilon^{-\frac{1}{3}}r^{\frac{2}{3}}, \tag{1.5}$$

and the θ-spectrum function

$$F(k) = n\chi\epsilon^{-1/3}k^{-5/3}. \tag{1.6}$$

q and n are dimensionless constants. Obukhov[39] and Corrsin[40] estimated the "cutoff" wavenumber for the convective subrange as $k_c = (\epsilon/\mathfrak{D}^3)^{\frac{1}{4}}$, where $\mathfrak{D}$ is the molecular diffusivity. However, Batchelor[41] argued that this cutoff wavenumber is permissible only for small Schmidt numbers $(\nu/\mathfrak{D}) \leq 1$. For large Schmidt numbers $(\nu/\mathfrak{D}) \gg 1$, Batchelor[41] suggested that there exists a viscous–convective subrange $[(\epsilon/\nu^3)^{\frac{1}{4}} \ll k \ll (\epsilon/\nu\mathfrak{D}^2)^{\frac{1}{4}}]$ and viscous diffusive subrange $[\{\epsilon/(\nu\mathfrak{D}^2)\}^{\frac{1}{4}} \ll k]$. He proposed a uniform straining model for these ranges and obtained the spectrum function

$$F(k) = -\chi\gamma^{-1}k^{-1}\exp\left\{\frac{\mathfrak{D}}{\gamma}k^2\right\}, \qquad k \gg k_K, \tag{1.7}$$

where $\gamma = -\frac{1}{2}(\epsilon/\nu)^{\frac{1}{2}}$. For small Schmidt number $(\nu/\mathfrak{D}) < 1$, Batchelor, Howells, and Townsend[42] proposed that there exists an inertial diffusive subrange and obtained

$$F(k) \approx \tfrac{1}{3}\chi\epsilon^{2/3}\mathfrak{D}^{-3}k^{-17/3}, \qquad k_c \ll k \ll k_K. \tag{1.8}$$

The scalar spectra in the universal range was further studied by Corrsin.[43,44] He applied Onsager's spectral jump concept for turbulent dynamics, as well as the concepts introduced by Batchelor[41] and Batchelor *et al.*,[42] to turbulent mixing with irreversible first-order reaction. Pao[45] further modified the concepts for scalar spectral transfer and made them adaptable for predicting the spectra for a turbulent multicomponent mixture with any type of isothermal first-order reaction. Recently, Corrsin[46] extended these concepts to the problems of turbulent mixing with second-order chemical reaction.

In this analysis, we shall propose a *simple* continuous spectral cascading process for transfer of turbulent kinetic energy, heat, and mass at large wavenumbers. Based on this concept, an energy spectrum function for the whole universal equilibrium range is deduced in closed form in Sec. II. The corresponding one-dimensional energy-spectrum functions are compared with measurements in Sec. III; they are in good agreement. In Sec. IV the temperature and concentration spectrum functions for the universal equilibrium ranges are deduced by using the same concept. The corresponding one-dimensional temperature and concentration spec-

[35] R. H. Kraichnan, J. Fluid Mech. **5**, 497 (1959).
[36] R. H. Kraichnan, and E. A. Spiegel, Phys. Fluids **5**, 583 (1962).
[37] S. F. Edwards, J. Fluid Mech. **18**, 239 (1964).
[38] R. H. Kraichnan, Phys. Fluids **7**, 1723 (1964): **8**, 575 (1965): **8**, 995 (1965).
[39] A. M. Obukhov, Izv. Akad. Nauk. SSSR Ser Geogr. i Geofiz. **13**, 58 (1949).
[40] S. Corrsin, J. Appl. Phys. **22**, 469 (1951).
[41] G. K. Batchelor, J. Fluid Mech. **5**, 113 (1959).
[42] G. K. Batchelor, I. D. Howells, and A. A. Townsend, J. Fluid Mech. **5**, 134 (1959).
[43] S. Corrsin, J. Fluid Mech. **11**, 407 (1961).
[44] S. Corrsin, *Proceedings of the 1961 Symposium on Fluid Dynamics and Applied Mathematics, University of Maryland* (Gordon and Breach Science Publishers, New York, 1962), pp. 105–124.
[45] Y. H. Pao, AIAA J. **2**, 1550 (1964).
[46] S. Corrsin, Phys. Fluids **7**, 1156 (1964).

trum functions are compared with measurements in Sec. V.

II. TRANSFER OF TURBULENT ENERGY AT LARGE WAVENUMBERS

Assuming isothermal constant density flow, the governing equations are:

the Navier–Stokes equations

$$\frac{\partial U_i}{\partial t} + U_j \frac{\partial U_i}{\partial x_j} = -\frac{1}{\rho}\frac{\partial P}{\partial x_i} + \nu \frac{\partial^2 U_i}{\partial x_j^2}, \tag{2.1}$$

the continuity equation

$$\partial U_i/\partial x_i = 0, \tag{2.2}$$

where U_i is the velocity vector, P is the pressure, ρ is the constant density, ν is the constant kinematic viscosity. For turbulent flow, each variable can be split into two parts: $U_i = \overline{U_i} + u_i$, $P = \overline{P} + p$. A bar denotes the ensemble average, $\overline{U_i}$ and $\overline{P}$ are the ensemble mean of the velocity and pressure fields, respectively. u_i and p are the fluctuations about their respective means; thus $\overline{u_i} = 0$, $\overline{p} = 0$. Assuming the flow is stationary, taking the ensemble mean of (2.1) gives the equations of mean motion,

$$\overline{U_j}\frac{\partial}{\partial x_j}\overline{U_i} + \overline{u_j \frac{\partial u_i}{\partial x_j}} = -\frac{1}{\rho}\frac{\partial \bar{P}}{\partial x_i} + \nu \frac{\partial^2}{\partial x_j^2}\overline{U_i}, \tag{2.3}$$

and the mean value of the continuity equation (2.2) is

$$\partial \overline{U_i}/\partial x_i = 0. \tag{2.4}$$

Subtracting these equations from the original ones, it is obtained that

$$\frac{\partial u_i}{\partial t} + u_j \frac{\partial u_i}{\partial x_j} = -\frac{1}{\rho}\frac{\partial p}{\partial x_i} + \nu \frac{\partial^2 u_i}{\partial x_j^2} + \overline{\frac{\partial u_i u_j}{\partial x_j}} - u_j \frac{\partial \overline{U_i}}{\partial x_j} - \overline{U_j}\frac{\partial u_i}{\partial x_j}, \tag{2.5}$$

$$\partial u_i/\partial x_i = 0. \tag{2.6}$$

Kolmogorov's hypothesis[1] asserts that the small-scale structure of turbulence is statistically steady and isotropic (thus, locally homogeneous). It implies that the statistical quantities $\overline{u_i u_j}$ $(\mathbf{x}, t)$ and $\overline{U_i}$ $(\mathbf{x}, t)$ do not vary appreciably in a small region (with characteristic length l_v); i.e.,

$$\frac{\partial}{\partial x_j}\overline{u_i u_j} = 0, \qquad \frac{\partial}{\partial x_j}\overline{U_i} = 0, \quad \text{for} \quad |\mathbf{x}' - \mathbf{x}| < l_v.$$

Furthermore, let the observer move with mean velocity $\overline{U_j}$, (2.5) and (2.6) reduce to

$$\frac{\partial u_i}{\partial t} + u_j \frac{\partial u_i}{\partial x_j} = -\frac{1}{\rho}\frac{\partial p}{\partial x_i} + \nu \frac{\partial^2 u_i}{\partial x_j^2}, \qquad |\mathbf{x}' - \mathbf{x}| < l_v, \tag{2.7}$$

$$\partial u_i/\partial x_i = 0. \tag{2.8}$$

(2.7) is the same form as the governing equation of homogeneous turbulence, but it is restricted to a limited region $|\mathbf{x}' - \mathbf{x}| < l_v$. The covariance equation of $\mathbf{u}$ can be formed in the usual way,[2] with local homogeneity, as

$$\frac{\partial}{\partial r_k}\left(\overline{u_i u_k' u_j'} - \overline{u_i u_k u_j'}\right) + \frac{1}{\rho}\left(\overline{\frac{\partial p' u_i}{\partial r_j}} - \overline{\frac{\partial p u_j'}{\partial r_i}}\right) = 2\nu \frac{\partial^2}{\partial r_k^2}\overline{u_i u_j'}, \qquad |\mathbf{x}' - \mathbf{x}| < l_v, \tag{2.9}$$

where the term $(\partial/\partial t)\,\overline{u_i u_j'} = 0$, as the flow is assumed to be stationary. $'$ denotes the field variable at $\mathbf{x}'$, e.g., $\mathbf{u}' = \mathbf{u}'(\mathbf{x}', t)$. With isotropy, (2.9) can be reduced to[2]

$$-\frac{1}{2}\left(r\frac{\partial}{\partial r} + 3\right)K(r) = 2\nu\left(\frac{\partial^2}{\partial r^2} + \frac{2}{r}\frac{\partial}{\partial r}\right)R(r), \tag{2.10}$$

where

$$2R(r) = \overline{u_i u_i'},$$

$$-\frac{1}{2}\left(r\frac{\partial}{\partial r} + 3\right)K(r) = \frac{\partial}{\partial r_k}\left(\overline{u_i u_k' u_i'} - \overline{u_i u_k u_i'}\right),$$

and the terms $(\partial/\partial r_i)\overline{p' u_i}$ and $(\partial/\partial r_i)\overline{p u_i'}$ are identically zero for locally isotropic turbulence. (2.10) can be transformed to wavenumber space as[2]

$$T(k) = 2\nu k^2 E(k), \tag{2.11}$$

where

$$T(k) = \frac{2}{\pi}\int_0^\infty \frac{1}{2}\left(r\frac{\partial}{\partial r} + 3\right)K(r) kr \sin kr\, dr,$$

$$E(k) = \frac{2}{\pi}\int_0^\infty R(r) kr \sin kr\, dr.$$

$T(k)$ represents the contribution due to inertial transfer of energy from all wavenumbers. Then, the energy flux from wavenumbers less than k to wavenumbers greater than k is

$$S(k) = \int_k^\infty T(k)\, dk. \tag{2.12}$$

Thus,

$$-dS(k)/dk = T(k). \tag{2.13}$$

In this section we propose an energy transfer mechanism for turbulent flows with very large Reynolds numbers; it leads to a relation between $T(k)$ amd $E(k)$. We visualize the transfer of turbulent energy as a cascading process in which the spectral elements are continuously transferred to ever larger wavenumbers. Following the migration of a spectral element initially at wavenumber k and time τ, the spectral element is transferred to a larger wavenumber k' at some instant $\Delta\tau$ later (as shown in Fig. 1). Let the rate that an energy spectral element is transferred across k be $\sigma(q) = dk/d\tau$; then, the energy flux across k is $E(k)\sigma(k) = S(k)$. We assert that the cascading rate of spectral element $\sigma(k)$ is dependent on ϵ (the rate that the turbulent energy is fed to the small eddies from the large eddies) and on the wavenumber k (or, equivalently, the size of the small eddies). Dimensional reasoning gives

$$\sigma(k) = \alpha^{-1}\epsilon^{1/3}k^{5/3}. \tag{2.14}$$

Thus,

$$S(k) = E(k)\sigma(k) = \alpha^{-1}\epsilon^{1/3}k^{5/3}E(k). \tag{2.15}$$

Combining (2.11)–(2.15), we have

$$-\frac{d}{dk}(\alpha^{-1}\epsilon^{1/3}k^{5/3}E) = 2\nu k^2 E.$$

Consequently,

$$E(k) = Nk^{-5/3}\exp(-\tfrac{3}{2}\alpha\nu\epsilon^{-1/3}k^{4/3}), \quad k \gg k_0, \tag{2.16}$$

where

$$N = E(k_*)k_*^{5/3}\exp(\tfrac{3}{2}\alpha\nu\epsilon^{-1/3}k_*^{4/3}).$$

k_* is any wavenumber in the universal range. A more convenient way to determine the constant N is by using the relation

$$\epsilon = 2\nu\int_0^\infty k^2E(k)\,dk$$

$$\approx 2\nu\int_0^\infty Nk^{1/3}\exp(-\tfrac{3}{2}\alpha\nu\epsilon^{-1/3}k^{4/3})\,dk.$$

Let $p = \frac{3}{2}\alpha\nu\epsilon^{-1/3}k^{4/3}$; then

$$\epsilon \approx N\alpha^{-1}\epsilon^{\frac{1}{3}}[e^{-p}]_\infty^0 = N\alpha^{-1}\epsilon^{\frac{1}{3}}.$$

Hence, $N \approx \alpha\epsilon^{2/3}$.

For very large Reynolds numbers, $N = \alpha\epsilon^{2/3}$. Thus, (2.16) can be rewritten as

$$E(k) = \alpha\epsilon^{2/3}k^{-5/3}\exp(-\tfrac{3}{2}\alpha\nu\epsilon^{-1/3}k^{4/3}), \quad k \gg k_0. \tag{2.17}$$

α is the Kolmogorov constant. The deduced energy spectrum function has no adjustable constant and is for the whole universal range $k \gg k_0$. Dividing (2.17) through by $\epsilon^{1/4}\nu^{5/4}$, a dimensionless relation is obtained:

$$\tilde{E}(\tilde{k}) = \alpha\tilde{k}^{-5/3}\exp(-\tfrac{3}{2}\alpha\tilde{k}^{4/3}), \quad \tilde{k} \gg \tilde{k}_0, \tag{2.18}$$

where $\tilde{E}(\tilde{k}) = E(k)/(\epsilon\nu^5)^{1/4}$ and $\tilde{k} = k/k_K$. In the inertial subrange $\tilde{k}_0 \ll \tilde{k} \ll 1$, (2.18) reduces to

$$\tilde{E}(\tilde{k}) = \alpha\tilde{k}^{-5/3}, \tag{2.19}$$

provided $\alpha = O(1)$. Eq. (2.19) can also be written as

$$E(k) = \alpha\epsilon^{2/3}k^{-5/3}, \quad k_0 \ll k \ll k_K,$$

which agrees with Kolmogorov's prediction (1.4). The Kolmogorov constant α, evaluated from a number of measurements, is somewhat scattered; the measurements by Grant, *et al.*,[21] in tidal streams ($R_\lambda \sim 2000$) give $\alpha = 1.22 \sim 1.81$ with a mean of $\alpha = 1.44$; Gibson's[23] measurements in round jet give $\alpha = 1.57$ at jet axis and $\alpha = 1.62$ at half radius ($R_\lambda \sim 800$). Obukhov[47] and Kolmogorov[48] recently refined the original Kolmogorov's hypothesis; they took into consideration the effects due to the intermittancy of the high-frequency turbulent fluctuation and the finite Reynolds numbers. One cannot tell whether these effects are present from the accuracy of the measurements reported so far. (The author is indebted to S. Corrsin for discussion on this point.) The energy spectrum function (2.18) is plotted in Fig. 2 for $\alpha = 1.5$.

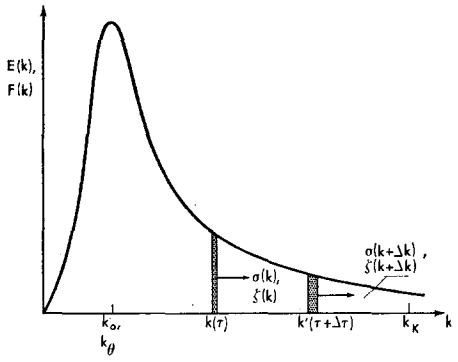

FIG. 1. Continuous cascading process of a spectral element.

The one-dimensional form of $E(k)$, $\varphi(k_1)$, is compared with measurements in the next section.

III. COMPARING THE ONE-DIMENSIONAL ENERGY SPECTRA WITH MEASUREMENTS

One-dimensional energy spectrum functions, $\varphi(k_1)$, have been measured in various turbulent flows.

[47] A .M. Obukhov, J. Geophys. Res. **67**, 3011 (1962); also J. Fluid Mech. **13**, 77 (1962).
[48] A. N. Kolmogorov, J. Fluid Mech. **13**, 82 (1962).

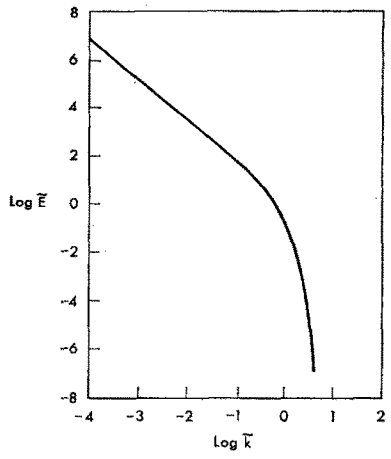

FIG. 2. Deduced energy spectrum in the universal equilibrium range.

$\varphi(k_1)$ is related to the three-dimensional energy spectrum function $E(k)$ as [49]

$$\varphi(k_1) = \int_{k_1}^{\infty} \left(1 - \frac{k_1^2}{k^2}\right) \frac{E(k)}{k}\, dk, \tag{3.1}$$

where $\varphi(k_1)$ is related to the turbulent energy as

$$\int_0^{\infty} \varphi(k_1)\, dk_1 = \langle u_1^2 \rangle. \tag{3.2}$$

It should be noted that the definition of $\varphi(k_1)$ is not uniform in the literature; the forms (3.1) and (3.2) are commonly used in experimental work. Some works[2] have used a $\varphi(k_1)$ which is half as large as that defined above. Dividing (3.1) through by $\epsilon^{1/4}\nu^{5/4}$, we have

$$\tilde{\varphi}(\tilde{k}_1) = \frac{\varphi(k)}{\epsilon^{1/4}\nu^{5/4}} = \int_{\tilde{k}_1}^{\infty} \left(1 - \frac{\tilde{k}_1^2}{\tilde{k}^2}\right) \frac{\tilde{E}(\tilde{k})}{\tilde{k}}\, d\tilde{k}. \tag{3.3}$$

Combining the predicted energy spectrum function (2.18) and (3.3), we obtain

$$\tilde{\varphi}(\tilde{k}_1) = \alpha \int_{\tilde{k}_1}^{\infty} \left(1 - \frac{\tilde{k}_1^2}{\tilde{k}^2}\right) \tilde{k}^{-8/3} \exp\left(-\tfrac{3}{2}\alpha \tilde{k}^{4/3}\right) d\tilde{k}, \qquad \tilde{k} \gg \tilde{k}_0. \tag{3.4}$$

Equation (3.4) can be transformed into a form which is more convenient for numerical integration by letting $\xi = \tilde{k}_1/\tilde{k}$:

$$\tilde{\varphi}(\tilde{k}_1) = \alpha \tilde{k}_1^{-5/3} \int_0^1 (1 - \xi^2)\xi^{2/3} \cdot \exp\left[-\tfrac{3}{2}\alpha\left(\frac{\tilde{k}_1}{\xi}\right)^{4/3}\right] d\xi. \tag{3.5}$$

This can be integrated numerically for given Kolmogorov's constant α.

Before comparing the numerical results of (3.5) with measurements, it should be re-emphasized that the energy spectrum functions (2.23) or (3.5) are deduced for turbulent flow with very large Reynolds numbers ($R_\lambda > 1000$, say). Strictly speaking, we cannot compare the deduced spectra with those spectra measurements in flows with moderate Reynolds numbers. To illustrate this point, a deduced spectral curve and a spectral curve measured in moderate Reynolds number flow are drawn schematically in Fig. 3. Their corresponding dissipation spectra are shown in Fig. 4. ϵ is related to $\varphi(k_1)$ as[49]

$$\epsilon = 15\nu \int_0^{\infty} k^2 \varphi(k)\, dk. \tag{3.6}$$

It is then obvious from Fig. 4 that at finite Reynolds numbers the ϵ used for theoretical deduction is greater than that measured; i.e., $\epsilon > \epsilon_{meas}$. This has been pointed out by Gibson and Schwarz.[24] Observations show that $\epsilon_{meas} \approx \epsilon$ for large enough Reynolds number. To estimate the difference between ϵ and ϵ_{meas} for a given turbulent flow, we can use the relation

$$\epsilon = 15\nu \int_0^{\infty} k^2 \varphi(k)\, dk = \epsilon_1 + \epsilon_2, \tag{3.7}$$

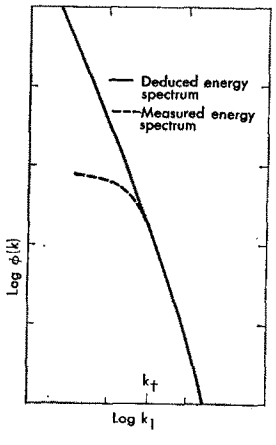

FIG. 3. The difference between deduced and measured energy spectra at small wavenumbers.

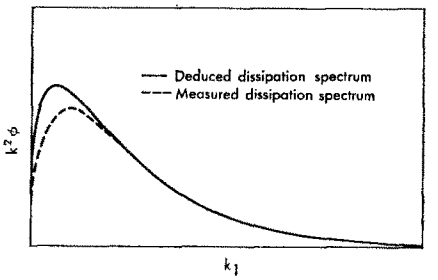

FIG. 4. The difference between deduced and measured dissipation spectra at small wavenumbers.

[49] J. O. Hinze, *Turbulence* (McGraw-Hill Book Company, New York, 1959), Chap. 3.

TABLE I. Deduced one-dimensional energy spectrum function.

$\tilde{k}_1$	$\tilde{\phi}$			$\tilde{k}_1$	$\tilde{\phi}$		
	$\alpha = 1.44$	$\alpha = 1.60$	$\alpha = 1.70$		$\alpha = 1.44$	$\alpha = 1.60$	$\alpha = 1.70$
1.0×10^{-4}	2.187×10^{6}	2.430×10^{6}	2.582×10^{6}	5.0×10^{-1}	2.016×10^{-1}	1.891×10^{-1}	1.811×10^{-1}
2.0×10^{-4}	6.888×10^{5}	7.654×10^{5}	8.132×10^{5}	6.0×10^{-1}	9.848×10^{-2}	8.920×10^{-2}	8.360×10^{-2}
4.0×10^{-4}	2.169×10^{5}	2.410×10^{5}	2.560×10^{5}	7.0×10^{-1}	5.030×10^{-2}	4.398×10^{-2}	4.033×10^{-2}
6.0×10^{-4}	1.103×10^{5}	1.225×10^{5}	1.302×10^{5}	8.0×10^{-1}	2.653×10^{-2}	2.238×10^{-2}	2.007×10^{-2}
8.0×10^{-4}	6.828×10^{4}	7.586×10^{4}	8.059×10^{4}	9.0×10^{-1}	1.433×10^{-2}	1.165×10^{-2}	1.022×10^{-2}
1.0×10^{-3}	4.705×10^{4}	5.228×10^{4}	5.554×10^{4}	1.0	7.885×10^{-3}	6.179×10^{-3}	5.297×10^{-3}
2.0×10^{-3}	1.479×10^{4}	1.642×10^{4}	1.745×10^{4}	1.2	2.480×10^{-3}	1.802×10^{-3}	1.474×10^{-3}
4.0×10^{-3}	4.636×10^{3}	5.146×10^{3}	5.465×10^{3}	1.4	8.086×10^{-4}	5.434×10^{-4}	4.235×10^{-4}
6.0×10^{-3}	2.345×10^{3}	2.602×10^{3}	2.763×10^{3}	1.6	2.695×10^{-4}	1.671×10^{-4}	1.239×10^{-4}
8.0×10^{-3}	1.443×10^{3}	1.601×10^{3}	1.698×10^{3}	1.8	9.109×10^{-5}	5.203×10^{-5}	3.666×10^{-5}
1.0×10^{-2}	9.892×10^{2}	1.096×10^{3}	1.162×10^{3}	2.0	3.104×10^{-5}	1.629×10^{-5}	1.089×10^{-5}
2.0×10^{-2}	3.013×10^{2}	3.328×10^{2}	3.523×10^{2}	2.2	1.062×10^{-5}	5.117×10^{-6}	3.241×10^{-6}
4.0×10^{-2}	8.817×10^{1}	9.675×10^{1}	1.020×10^{2}	2.4	3.644×10^{-6}	1.605×10^{-6}	9.629×10^{-7}
6.0×10^{-2}	4.152×10^{1}	4.525×10^{1}	4.752×10^{1}	2.6	1.249×10^{-6}	5.027×10^{-7}	2.849×10^{-7}
8.0×10^{-2}	2.376×10^{1}	2.571×10^{1}	2.688×10^{1}	2.8	4.271×10^{-7}	1.567×10^{-7}	8.387×10^{-8}
1.0×10^{-1}	1.512×10^{1}	1.625×10^{1}	1.692×10^{1}	3.0	1.455×10^{-7}	4.862×10^{-8}	2.453×10^{-8}
2.0×10^{-1}	3.175×10^{0}	3.299×10^{0}	3.365×10^{0}	3.2	4.939×10^{-8}	1.498×10^{-8}	7.124×10^{-9}
3.0×10^{-1}	1.073×10^{0}	1.078×10^{0}	1.077×10^{0}	3.4	1.667×10^{-8}	4.590×10^{-9}	2.052×10^{-9}
4.0×10^{-1}	4.413×10^{-1}	4.284×10^{-1}	4.190×10^{-1}				

where

$$\epsilon_1 = 15\nu \int_0^{k^\dagger} k^2 \varphi(k)\, dk, \tag{3.8}$$

$$\epsilon_2 = 15\nu \int_{k^\dagger}^{\infty} k^2 \varphi(k)\, dk, \tag{3.9}$$

where $k_\dagger$ is the wavenumber at which the spectrum begins to deviate from $k^{-5/3}$ (as shown in Fig. 3). Thus, $\epsilon_1 > (\epsilon_1)_{\text{meas}}$, $\epsilon_2 = (\epsilon_2)_{\text{meas}}$. Combining (2.10), (3.8), and (3.9), we obtain

$$\epsilon_1 = 2\nu\alpha\epsilon^{2/3} \int_0^{k^\dagger} k^{1/3} \exp\left(-\tfrac{3}{2}\alpha\nu\epsilon^{-1/3}k^{4/3}\right) dk$$

$$= \epsilon[\exp\left(-\tfrac{3}{2}\alpha\tilde{k}^{4/3}\right)]_{\tilde{k}^\dagger}^{0} > (\epsilon_1)_{\text{meas}}, \tag{3.10}$$

$$\epsilon_2 = 2\nu\alpha\epsilon^{2/3} \int_{k^\dagger}^{\infty} k^{1/3} \exp\left(-\tfrac{3}{2}\alpha\nu\epsilon^{-1/3}k^{4/3}\right) dk$$

$$= \epsilon[\exp\left(-\tfrac{3}{2}\alpha\tilde{k}^{4/3}\right)]_{\infty}^{\tilde{k}^\dagger} = (\epsilon_2)_{\text{meas}}. \tag{3.11}$$

For small enough $k_\dagger$, $\epsilon_2 \to \epsilon$ and $\epsilon_1 \to 0$. Since $\epsilon_{\text{meas}} = (\epsilon_1)_{\text{meas}} + (\epsilon_2)_{\text{meas}}$, $(\epsilon/\epsilon_{\text{meas}}) < (\epsilon/\epsilon_2)$. Therefore, ϵ/ϵ_2 gives an upper limit for $\epsilon/\epsilon_{\text{meas}}$. From (3.11),

$$\epsilon/\epsilon_2 = \exp\left(\tfrac{3}{2}\alpha\tilde{k}_\dagger^{4/3}\right) > \epsilon/\epsilon_{\text{meas}}. \tag{3.12}$$

Measurements show that for large Reynolds number ($R_\lambda \sim 2000$, say) $\tilde{k}_\dagger = (k_\dagger/k_K) \sim 10^{-3}$; with $\alpha = 1.5$; $(\epsilon/\epsilon_2) = \exp(2.25 \times 10^{-4}) \sim (1 + 10^{-3}) > (\epsilon/\epsilon_{\text{meas}})$; thus ϵ differs very little from ϵ_{meas}. However, for moderate Reynolds numbers the spectra deviate from $\tilde{k}^{-5/3}$ at larger $\tilde{k}$, $\tilde{k}_\dagger = 10^{-1}$, say, then $(\epsilon/\epsilon_2) = \exp(2.25 \times 10^{-4/3}) = 1.11$. Thus ϵ could be larger than ϵ_{meas} by as much as 10% of ϵ_{meas}. This means that the theoretical flow is significantly different from the experimental flow. The usual nondimensionalized energy spectra, $\varphi/(\epsilon^{1/4}\nu^{5/4})$, only depend on ϵ to the one-fourth power. The difference between $\epsilon^{1/4}$ and $\epsilon_{\text{meas}}^{1/4}$ may be considered negligible even for spectra measurements at moderate Reynolds number. However, to bring out the features of energy spectra at very large wavenumbers (dissipation subrange, $k \geq k_K$), the measurements have been presented as $\tilde{k}^2\tilde{\varphi}$, $\tilde{k}^4\tilde{\varphi}$, and $\tilde{k}^6\tilde{\varphi}$ vs $\tilde{k}$. Take the case of $\tilde{k}^6\tilde{\varphi}$ vs $\tilde{k}$,

$$k^6\tilde{\phi} = \left[\frac{k}{(\epsilon/\nu^3)^{1/4}}\right]^6 \frac{\varphi}{\epsilon^{1/4}\nu^{5/4}} = \frac{k^6\varphi}{\epsilon^{7/4}\nu^{-13/4}}. \tag{3.13}$$

Then the differences between ϵ and ϵ_{meas} become important and flows with large Reynolds numbers are required. This is why, among other reasons to be discussed later, one has to be very cautious in comparing present results with the spectra measurements of $\tilde{k}^4\tilde{\varphi}$ vs $\tilde{k}$ and $\tilde{k}^6\tilde{\varphi}$ vs $\tilde{k}$ in the dissipation range ($k \geq k_K$) of turbulent flows with moderate Reynolds numbers, such as the spectra measurements by Stewart and Townsend[12] and Liepmann, Laufer, and Liepmann[14] ($R_\lambda < 30$).

Relation (3.5) is integrated numerically and tabulated for $\alpha = 1.44$, 1.60, and 1.70 in Table I (more detailed results are tabulated in Ref. 50 for $\alpha = 1.44$, 1.50, 1.60 and 1.70). Comparing the deduced spectra with the measured energy spectra of turbulent flows with very large Reynolds number by Grant, Stewart,

[50] Yih-Ho Pao, Boeing Document D1-82-0369, 1964.

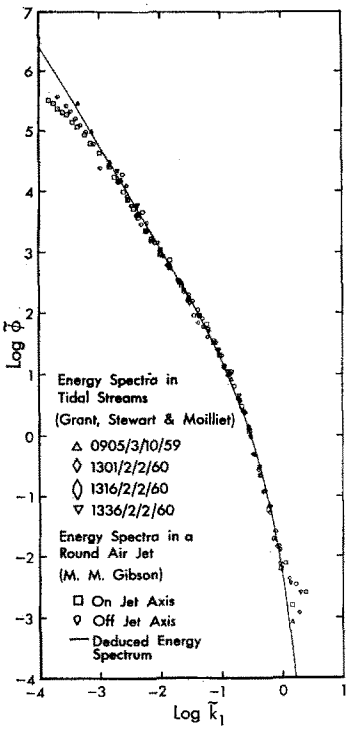

FIG. 5. Deduced and measured one-dimensional energy spectra.

and Moilliet[21] ($R_\lambda \sim 2000$) and Gibson[23] ($R_\lambda \sim 800$) (the author is indebted to M. M. Gibson for furnishing the tabulated spectral data), it is found that $\alpha = 1.7$ gives the best agreement. These are plotted as log $\tilde{\varphi}$ vs log $\tilde{k}_1$ in Fig. 5. To emphasize the energy spectral behavior at very large wavenumbers, the deduced spectrum is compared with measurements as $\tilde{k}_1^2\tilde{\varphi}$ vs $\tilde{k}_1$ in Fig. 6 and $\tilde{k}_1^4\tilde{\varphi}$ vs $\tilde{k}_1$ in Fig. 7. Unfortunately, energy spectra measurements in the dissipation subrange $k \geq k_K$, especially in flows with very large Reynolds numbers, are hampered by experimental difficulties.[51,52] Turbulent energy spectra have mostly been measured with hot-wire or hot-film anemometers, its frequency response is limited by its electronics, and by the finite length of hot wires or hot films. The size restriction is inherent, but can be somewhat relaxed with the wire-length correction formula deduced by Uberoi and Kovasznay.[53] Furthermore, the noise of the hot-wire or hot-film anemometer is increasing with frequency. Therefore, the noise is increasing with wavenumber ($k = 2\pi f/U$ by Taylor's hypothesis). The signal and noise become indistinguishable at large enough wavenumbers. The errors of measurements at very large wavenumbers are magnified in the $\tilde{k}_1^4\tilde{\varphi}$ vs $\tilde{k}_1$ plot, as shown in Fig. 7, where the measured values are quite scattered beyond $k_1 > k_K$.

Lacking acceptable energy spectral measurements for $k_1 \geq k_K$ in flows with large Reynolds numbers, we shall compare our deduced $\tilde{\varphi}$ with spectral data of Stewart and Townsend[12] which were taken in turbulent flows with moderate Reynolds numbers ($R_\lambda < 30$). As was pointed out by Stewart and Townsend,[12] the absolute values of their measured spectra were not certain, although the relative values were believed to be accurate. Furthermore, owing to the low-turbulence Reynolds number, the difference between ϵ and ϵ_{meas} becomes appreciable in the $\tilde{k}_1^6\tilde{\varphi}$ vs $\tilde{k}_1$ plot as discussed previously. With these reservations in mind, we have plotted in Fig. 8 the deduced one-dimensional energy spectrum and the data of Stewart and Townsend[12] as $\tilde{k}_1^6\tilde{\varphi}$ vs $\tilde{k}_1$,

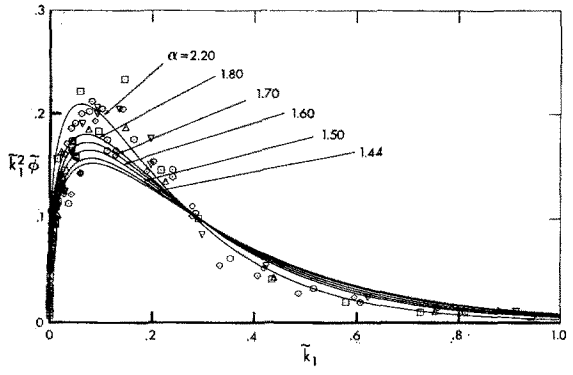

FIG. 6. Comparison of deduced $\tilde{k}^2\tilde{\varphi}$ vs $\tilde{k}$ with data of Grant, Stewart and Moilliet (Ref. 21), and Gibson (Ref. 23).

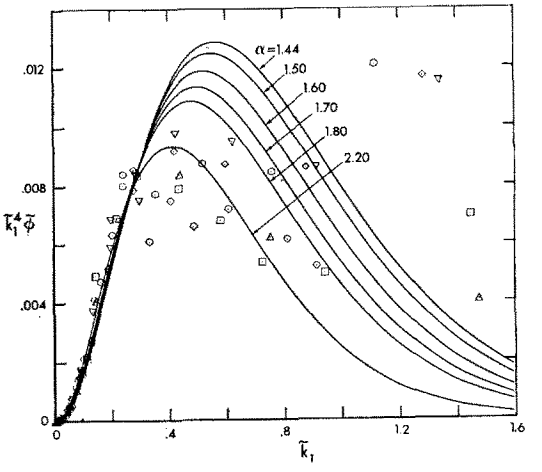

FIG. 7. Comparison of Deduced $\tilde{k}^4\tilde{\varphi}$ vs $\tilde{k}$ with data of Grant, Stewart, and Moilliet (Ref. 21); and Gibson (Ref. 23).

[51] L. S. G. Kovasznay, in *High Speed Aerodynamics and Jet Propulsion* (Princeton University Press, Princeton, New Jersey, 1954), Vol. 9, Sec. F.

[52] S. Corrsin, in *Encyclopedia of Physics*, Fluid Dynamics II (Springer-Verlag, Berlin, 1963), Vol. XIII/2, pp. 524–590.

[53] M. S. Uberoi, and L. S. G. Kovasznay, Quart. Appl. Math. **10**, 375 (1953).

they seem to have the same trend. For comparison, we have also plotted in Fig. 8 the Heisenberg and Kovasznay one-dimensional energy spectra which were computed by Reid.[33]

IV. TURBULENT TRANSFER OF SCALAR QUANTITIES AT LARGE WAVENUMBERS

The dilute diffusive scalar quantity $\Theta(\mathbf{x}, t)$—such as the concentration of a dilute species and the temperature—in a turbulent flow is governed by the convective diffusion equation,[49]

$$\frac{\partial\Theta}{\partial t} + U_i \frac{\partial\Theta}{\partial x_i} = \mathfrak{D} \frac{\partial^2\Theta}{\partial x_i^2}, \tag{4.1}$$

the equation of motion (2.1), and the continuity equation (2.2). Again, let us define $\Theta = \bar{\Theta} + \theta$; $\bar{\Theta}$ is the ensemble mean, and θ is the fluctuation about the mean. Assuming the scalar field is also stationary, the mean scalar quantity is governed by

$$\overline{U_i} \frac{\partial\bar{\Theta}}{\partial x_i} + \overline{u_i \frac{\partial\theta}{\partial x_i}} = \mathfrak{D} \frac{\partial^2\bar{\Theta}}{\partial x_i^2}. \tag{4.2}$$

Subtracting (4.2) from (4.1), it is obtained that

$$\frac{\partial\theta}{\partial t} + u_i \frac{\partial\theta}{\partial x_i} = \mathfrak{D} \frac{\partial^2\theta}{\partial x_i^2} - \overline{U_i} \frac{\partial\theta}{\partial x_i} - u_i \frac{\partial\bar{\Theta}}{\partial x_i} + \overline{u_i \frac{\partial\theta}{\partial x_i}}. \tag{4.3}$$

With a direct extension of Kolmogorov's hypotheses, the small-scale components of the scalar field are statistically steady and isotropic (thus homogeneous). Consequently, the quantities $\bar{\Theta}$ and $\overline{u_i\theta}$ are uniform in a small region (with characteristic length l_θ); thus $u_i(\partial/\partial x_i)\bar{\Theta} = 0$ and $(\partial/\partial x_i)\overline{u_i\theta} = 0$ for $|\mathbf{x}' - \mathbf{x}| < l_\theta$. Again, let the observer travel with velocity $\overline{U_i}$. (4.3) is reduced to

$$\frac{\partial\theta}{\partial t} + u_i \frac{\partial\theta}{\partial x_i} = \mathfrak{D} \frac{\partial^2\theta}{\partial x_i^2}, \qquad |\mathbf{x}' - \mathbf{x}| < l_\theta, \tag{4.4}$$

which is the same form as the governing equation for homogeneous turbulent mixing[49] but is restricted to a local region. The covariance equation for θ can be formed in the usual way[49] as

$$\overline{(u_i' - u_i) \frac{\partial}{\partial r_i} (\theta\theta')} = 2\mathfrak{D} \frac{\partial^2 \overline{\theta\theta'}}{\partial r_i^2}, \qquad |\mathbf{x}' - \mathbf{x}| < l_\theta. \tag{4.5}$$

where local homogeneity and local isotropy have been assumed. θ' is written for $\theta(\mathbf{x} + \mathbf{r}, t)$. $(\partial/\partial t)\cdot \overline{\theta\theta'} = 0$ because the θ-field is assumed stationary.

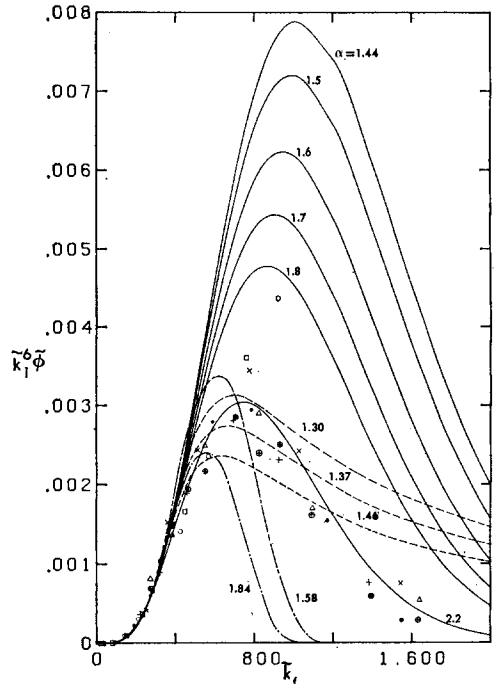

FIG. 8. Comparison of $\tilde{k}^6\tilde{\varphi}$ vs $\tilde{k}$ with data of Stewart and Townsend (Ref. 12). ———— present spectrum, - - - - - - - Heisenberg spectrum [after Reid (Ref. 33)], — — — — — Kovasznay spectrum [after Reid (Ref. 33)].

By transforming (4.5) to wavenumber space, one obtains[49]

$$Z(k) = 2\mathfrak{D}k^2F(k), \tag{4.6}$$

where

$$Z(\mathbf{x}) = \frac{2}{\pi}\int_0^\infty \overline{(u_i - u_i') \frac{\partial(\theta\theta')}{\partial r_i}} kr \sin kr\, dr,$$

$$F(k) = \frac{2}{\pi}\int_0^\infty \overline{\theta\theta'} kr \sin kr\, dr.$$

$Z(k)$ represents the contribution due to turbulent convective transfer of $\langle\theta^2\rangle$-content from all other wavenumbers. Thus, the $\langle\theta^2\rangle$-flux from wavenumbers less than k to wavenumbers greater than k is

$$Y(k) = \int_k^\infty Z(k)\, dk.$$

Hence,

$$-dY(k)/dk = Z(k). \tag{4.7}$$

As in the case of the energy transfer, we follow the migration of a scalar spectral element in the universal range, $k \gg k_\theta$ (also shown in Fig. 1). $k_\theta = L_\theta^{-1}$, where L_θ is the integral length scale of the scalar field. Let the rate that the scalar spectral element is transferred across k be $\zeta(k) = (d/d\tau)k$.

Then the scalar spectral flux across k is $Y(k) = F(k)\zeta(k)$. As the cascading of $\langle\theta^2\rangle$ content is mainly due to turbulent convection, which in turn is mainly dependent on the energy flux supplied by the large eddies ϵ, we assert that the cascading rate of $\langle\theta^2\rangle$ spectral element $\zeta(k)$ is again dependent upon ϵ and k. Dimensional reasoning gives

$$\zeta(k) = n^{-1}\epsilon^{1/3}k^{5/3}, \tag{4.8}$$

where n is a dimensionless constant. Therefore,

$$Y(k) = F(k)\zeta(k) = n^{-1}\epsilon^{1/3}k^{5/3}F(k). \tag{4.9}$$

Combining (4.6), (4.7), and (4.9), we obtain

$$-\frac{d}{dk}(n^{-1}\epsilon^{1/3}k^{5/3}F) = 2\mathfrak{D}k^2F.$$

Hence,

$$F(k) = Qk^{-5/3}\exp(-\tfrac{3}{2}n\mathfrak{D}\epsilon^{1/3}k^{4/3}), \tag{4.10}$$

where Q is a constant which can be determined as

$$Q = F(k_*)k_*^{5/3}\exp(\tfrac{3}{2}n\mathfrak{D}\epsilon^{-1/3}k_*^{4/3}).$$

Alternatively,

$$\chi = 2\mathfrak{D}\int_0^\infty k^2F(k)\,dk$$

$$\approx 2\mathfrak{D}\int_0^\infty Qk^{1/3}\exp(-\tfrac{3}{2}n\mathfrak{D}\epsilon^{-1/3}k^{4/3})\,dk.$$

Let

$$q = \tfrac{3}{2}n\mathfrak{D}\epsilon^{-1/3}k^{4/3},$$

$$\chi \approx Qn^{-1}\epsilon^{\frac{1}{3}}[\epsilon^{-q}]_\infty^0 = Qn^{-1}\epsilon^{\frac{1}{3}}.$$

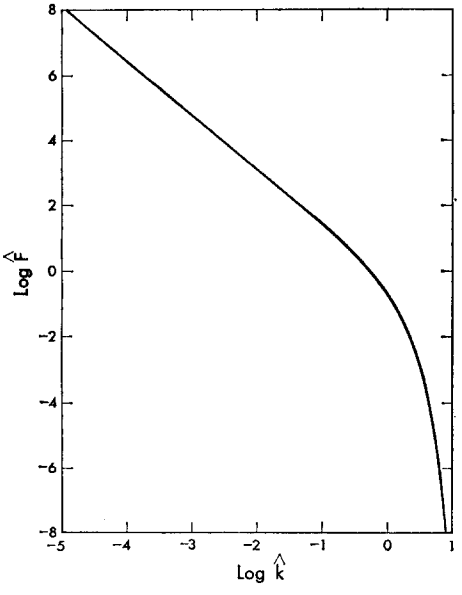

FIG. 9. Deduced scalar spectrum in the universal range, $n = 0.59$.

Thus,

$$Q \approx n\epsilon^{-\frac{1}{3}}\chi. \tag{4.11}$$

For very large Reynolds numbers and Péclet numbers, $Q = n\epsilon^{-1/3}\chi$; hence, (4.10) can be rewritten as

$$F(k) = n\chi\epsilon^{-1/3}k^{-5/3}\exp(-\tfrac{3}{2}n\mathfrak{D}\epsilon^{-1/3}k^{4/3}),$$

$$k \gg k_\theta; \tag{4.12}$$

n is a universal constant. Concentration and temperature spectra measurements in flow with moderate Reynolds numbers indicate that n is the order of unity. For more accurate determination of scalar spectra, measurements in flows with large Reynolds numbers ($R_\lambda \sim 1000$) are needed. Dividing (4.12) through by $\epsilon^{-3/4}\nu^{5/4}\chi$, we obtain

$$\tilde{F}(\tilde{k}) = \frac{F(k)}{\chi\epsilon^{-3/4}\nu^{5/4}} = n\tilde{k}^{-5/3}$$

$$\cdot\exp\left[-\tfrac{3}{2}n\left(\frac{\mathfrak{D}}{\nu}\right)\tilde{k}^{4/3}\right], \qquad \tilde{k} \gg \tilde{k}_\theta. \tag{4.13}$$

Alternatively, dividing (4.12) through by $\chi\epsilon^{-3/4}\mathfrak{D}^{5/4}$, we obtain

$$\hat{F}(\hat{k}) = \frac{F(k)}{\chi\epsilon^{-3/4}\mathfrak{D}^{5/4}} = n\hat{k}^{-5/3}\exp(-\tfrac{3}{2}n\hat{k}^{4/3}),$$

$$\hat{k} \gg \hat{k}_\theta, \tag{4.14}$$

where $\hat{k} = k/(\epsilon\mathfrak{D}^{-3})^{1/4}$. (4.14) is a very convenient universal form, which is plotted in Fig. 9 with $n = 0.59$. For $n = O(1)$ and $\hat{k} \ll 1$, (4.14) reduces to

$$\hat{F}(\hat{k}) = n\hat{k}^{-5/3}, \qquad \hat{k} \ll 1.$$

Or, equivalently,

$$F(k) = n\chi\epsilon^{-1/3}k^{-5/3} \qquad k \ll (\epsilon/\mathfrak{D}^3)^{1/4},$$

which agrees with the prediction of Corrsin by direct extension of Kolmogorov's hypothesis. Relation (4.12) has been obtained by Pao,[45] and independently by Corrsin,[46] as the scalar spectrum function in the inertial-diffusive subrange ($k_\theta \ll k \ll k_\epsilon$) for small Schmidt numbers, $(\nu/\mathfrak{D}) \leq 1$. The present arguments assert that (4.12) is the scalar spectrum function for the whole universal range, $k \gg k_\theta$, and for arbitrary Schmidt numbers. In obtaining (4.12), we have essentially postulated that the small-scale structure of θ is dependent on ϵ, χ, and $\mathfrak{D}$, but it is independent of ν. As a result, (4.12) differs from Batchelor's[41] prediction of $F(k)$ for large Schmidt number ($\nu/\mathfrak{D} \gg 1$) and Batchelor, Howells, and Townsend's[42] prediction of $F(k)$ for small Schmidt number ($\nu/\mathfrak{D} < 1$), where they have postulated

that $F(k)$ is dependent on ϵ, χ, $\mathfrak{D}$, and ν. For large Schmidt numbers, (4.12) differs from Batchelor's[41] result

$$F(k) \approx 2\chi\nu^{\frac{1}{2}}\epsilon^{-\frac{1}{2}}k^{-1} \cdot \exp(-2\mathfrak{D}\nu^{\frac{1}{2}}\epsilon^{-\frac{1}{2}}k^2), \qquad k \gg k_K, \tag{4.15}$$

which is the result of uniform straining approximation. Since

$$\langle\theta^2\rangle = \int_0^\infty F(k)\,dk = \int_0^{k_K} F(k)\,dk + \int_{k_K}^\infty F(k)\,dk, \tag{4.16}$$

from Batchelor's result (4.15),

$$\langle\theta^2\rangle = \int_0^{k_K} F(k)\,dk + \int_{k_K}^\infty \chi|\gamma|^{-1}k^{-1}\exp\left(-\frac{\mathfrak{D}}{|\gamma|}k^2\right)dk = \int_0^{k_K} F(k)\,dk + \tfrac{1}{2}\chi|\gamma|^{-1}\int_{\mathfrak{D}/|\gamma|k_K^2}^\infty \frac{e^{-n}}{n}\,dn = \int_0^{k_K} F(k)\,dk + \chi\nu^{\frac{1}{2}}\epsilon^{-\frac{1}{2}}\left|\mathrm{Ei}\left(-2\frac{\mathfrak{D}}{\nu}\right)\right|, \tag{4.17}$$

when $\mathfrak{D} \to 0$ in (4.17), $\langle\theta^2\rangle \to \infty$. Batchelor interpreted this difficulty as meaning that for $\mathfrak{D} = 0$ a statistically steady state for the small scale θ distribution is not possible for finite $\langle\theta^2\rangle$ content and for finite time. Batchelor estimated the time required for a scalar spectral element to travel from Kolmogorov wavenumber $k_K = (\epsilon/\nu^3)^{1/4}$ to $k_B = (\epsilon/\nu\mathfrak{D}^2)^{1/4}$ as

$$\Delta\tau = (\nu/\epsilon)^{\frac{1}{2}}\ln\nu/\mathfrak{D}. \tag{4.18}$$

Thus, it takes an infinitely long time for a spectral element to reach k_B when $\mathfrak{D} = 0$. Batchelor's arguments imply that the Reynolds number and the Péclet number of the turbulent flow must be very large for the small scale θ variations to achieve statistically universal steady state structure, but the Péclet number cannot be too large [$P = (u\lambda_\theta/\mathfrak{D}) \to \infty$ as $\mathfrak{D} \to 0$]; otherwise the steady state cannot be achieved. Furthermore, as the spectral element cascading rate is independent of $\mathfrak{D}$ in the convective subrange $k_\theta \ll k \ll k_K$, there can exist a steady state $k^{-5/3}$ range even if $\mathfrak{D} \to 0$ (by direct extension of Kolmogorov's hypotheses), provided that the Reynolds number and Péclet number are large enough. Therefore, Batchelor's results further imply that, as $\mathfrak{D} \to 0$, it is possible to have a steady state range at $k_\theta \ll k \ll k_K$ but nonsteady range at larger wavenumbers. It remains to be seen whether these consequences are valid. Unfortunately, θ-spectral measurements obtained so far are not conclusive enough to distinguish the differences between the present spectrum and Batchelor's spectrum. This point will be further discussed in the next section.

It can be shown that Batchelor's uniform straining concept[45] is equivalent to letting the spectral element cascading rate

$$\zeta(k) = 2\nu^{\frac{1}{2}}\epsilon^{-\frac{1}{2}}k.$$

It can also be shown that any $\zeta(k)$ faster than k [i.e., for $\zeta(k) \sim k^n$, $n > 1$] gives finite $\langle\theta^2\rangle$ regardless of diffusivity $\mathfrak{D}$. Therefore, if we admit that for large enough Reynolds numbers and Péclet numbers the statistical structures of small scale scalar fields are universal, regardless of $\mathfrak{D}$ and $\langle\theta^2\rangle$, it is likely that Batchelor's uniform straining model underestimates the turbulent straining rate and thus overestimates the concentration spectra.

Based on the preceding spectral cascade concept, the concentration spectra of a multicomponent mixture with isothermal first-order reactions obtained by Pao can be modified in a similar way; the reacting concentration spectra for the whole universal range can be obtained by solving (3.73) of Ref. 45.

V. COMPARING THE ONE-DIMENSIONAL SCALAR SPECTRUM FUNCTION WITH MEASUREMENTS

The one-dimensional scalar spectrum function, $\psi(k_1)$, which can be measured, is related to the three-dimensional scalar spectrum function as[49]

$$\psi(k_1) = \int_{k_1}^\infty \frac{F(k)}{k}\,dk. \tag{5.1}$$

Combining (5.1) and (4.12), we obtain

$$\psi(k_1) = n\chi\epsilon^{-1/3}\int_{k_1}^\infty k^{-8/3}\exp(-\tfrac{3}{2}n\mathfrak{D}\epsilon^{-1/3}k^{4/3})\,dk, \qquad k_1 \gg k_\theta. \tag{5.2}$$

Dividing (5.2) by $\epsilon^{-3/4}\mathfrak{D}^{5/4}\chi$, we have

$$\hat{\psi}(\hat{k}_1) = \frac{\psi(k_1)}{\epsilon^{-3/4}\mathfrak{D}^{5/4}\chi} = n\int_{\hat{k}_1}^\infty \hat{k}^{-8/3}\exp(-\tfrac{3}{2}n\hat{k}^{4/3})\,d\hat{k}, \qquad \hat{k}_1 \gg \hat{k}_\theta. \tag{5.3}$$

For numerical integration, we put $q = \hat{k}_1/\hat{k}$; thus,

$$\hat{\psi}(\hat{k}_1) = n\hat{k}_1^{-5/3}\int_0^1 q^{2/3}\exp\left[-\tfrac{3}{2}n\left(\frac{\hat{k}_1}{q}\right)^{4/3}\right]dq, \qquad \hat{k}_1 \gg \hat{k}_\theta. \tag{5.4}$$

The universal constant n has not been conclusively determined by measurements. We have integrated (5.4) numerically for $n = 0.59$.[24]

Measuring techniques for temperature and concentration fluctuations are not as well developed as those for velocity fluctuations. Furthermore, the scalar spectral data reported so far[10,54-59] have been measured in moderate Reynolds number flows ($R_\lambda < 120$); hence, similar to the discussion in Sec. III, ϵ and χ will differ appreciably from ϵ_{meas} and χ_{meas}. It is not possible then to compare the deduced scalar spectrum function (5.4) with the observations critically. Nevertheless, lacking better data, a few measured scalar spectra will be compared with the deduced results in this section.

Corrsin and Uberoi[10] have measured the temperature of a heated air jet at $x/d = 20$, both on the jet axis and at the maximum shear region, by using the constant current hot wire as a resistance thermometer. The data on the jet axis ($R_\lambda \sim 115$) will be used where the small perturbation hot-wire theory is expected to be moderately accurate. The data is reduced (details in Ref. 50) to dimensionless form, and plotted as log $\hat{\psi}$ vs log $\hat{k}$ in Fig. 10. It is in moderate agreement with the deduced spectrum for $n = 0.59$.

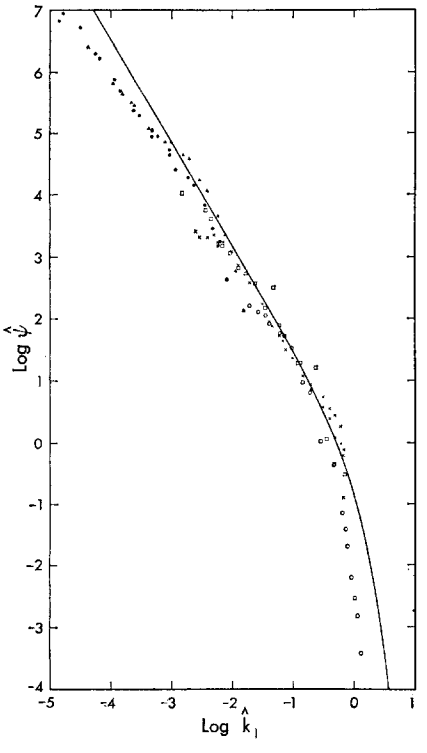

FIG. 10. Deduced and measured one-dimensional scalar spectra: × temperature spectrum in a round air jet (Corrsin and Uberoi); ○ temperature spectrum behind a heated grid in wind tunnel (Kistler, O'Brien, and Corrsin); □ temperature spectrum behind a heated grid in water tunnel (Gibson and Schwarz); ● CM-13, △ CM-15 concentration spectra behind a grid in water tunnel (Gibson and Schwarz); — deduced scalar spectrum.

Mills, Kistler, O'Brien, and Corrsin[54] have measured the temperature spectra behind a heated grid in a wind tunnel. Due to the low level of temperature fluctuation, the hot-wire temperature was set at the same order of response to velocity and temperature. Then, the temperature spectrum was obtained by subtracting the unheated grid velocity spectrum from the mixed spectrum. The temperature spectra data from their preliminary report[55] will be used. The spectra data is also reduced to log $\hat{\psi}$ vs log $\hat{k}$ (details in Ref. 50) and plotted in Fig. 10.

The measurements of temperature spectrum at high frequency (thus large wavenumbers) with constant current hot-wires are limited, as are the velocity spectrum measurements, by the wire length and anemometer noise. Furthermore, it is very difficult to find out the true frequency response characteristics (the response to temperature fluctuation versus frequency).

Gibson and Schwarz[24] have measured the temperature and salt concentration spectra behind grids in a water tunnel with the single-electrode conductivity probe. They have indicated that their measured scalar spectra shows the $k^{-5/3}$ inertial-convective subrange and also partially supports Batchelor's k^{-1} spectrum at larger wavenumbers. However, most of their scalar spectra were measured in flows with $R_\lambda < 55$ (the highest $R_\lambda = 70$, CM − 13). It is suspected that their R_λ are too low to have appreciable (over a decade, say) inertial-convective subrange. (Their spectral data are examined in detail in Ref. 50.) Careful examination of their data shows that their temperature spectral measurements ($\nu/\mathfrak{D} = 7$) are in fair agreement with our prediction (5.4). However, the slopes $d(\log \hat{\psi})/d(\log \hat{k})$ of their concentration spectral data ($\nu/\mathfrak{D} = 700$) are less then Batchelor's prediction, but greater than our prediction. The spectra data of their concentration measurements, CM − 13 ($R_\lambda \sim 70$), CM − 14 ($R_\lambda \sim 51$), and temperature measurements, TM − 2, are reduced and plotted in Fig. 10. Although Gibson and Schwarz have made significant advances for measuring the concentration and the temperature fluctuations with the single-electrode

[54] S. Corrsin, and M. S. Uberoi, NACA Report 998 (1950).
[55] R. R. Mills, Jr., A. L. Kistler, V. O'Brien, and S. Corrsin, NACA Technical Note 4288 (1958).
[56] A. L. Kistler, V. O'Brien, and S. Corrsin, NACA Research Memo 54D19 (1954).
[57] C. H. Gibson, Ph.D. thesis, Stanford University, Stanford, California (1962).
[58] H. A. Becker, H. C. Hottel, and G. C. Williams, Am. Inst. Chem. Eng. Annual Meeting, Paper No. 17D, Houston, Texas (1963).
[59] J. Lee, and R. S. Brodkey, Am. Inst. Chem. Eng. J. 10, 187 (1964).

conductivity probe, it should be cautioned that, in addition to the limitations due to probe size and instrument noise (as hot-wires), their measurements are further hampered by the unknown frequency-response characteristics, the unknown effects due to flow around the electrode and to probe support.

VI. FURTHER DISCUSSION ON THE CONTINUOUS SPECTRAL CASCADING PROCESS

The continuous spectral cascading concepts introduced for turbulent kinetic energy transfer (Sec. II) and for turbulent heat and mass transfer at large wavenumbers (Sec. IV) are, in essence, a modification and generalization of Onsager's[6] spectral jump concept. Onsager[6] visualizes the turbulent energy cascade as a geometric progression of wavenumber steps, doubling at each step; the time interval for a step is dependent on $E(k)$ and k. Onsager's spectral jump concept for turbulent energy was further extended to turbulent mixing by Corrsin.[43,44] In this analysis, we have visualized the turbulent energy, heat and mass spectral transfer as a continuous cascading process rather than discrete jumps; the spectral cascading rates, $\sigma(k)$ and $\zeta(k)$, are completely determined by the turbulent energy flux supplied by large scale-components, ϵ, and the wavenumber k; they are independent of the energy spectrum function $E(k)$ and the scalar spectrum function $F(k)$.

It should be kept in mind that the transfer of turbulent kinetic energy, heat, and mass among wavenumbers basically must be complicated processes. What we have attempted here is to represent them by simple continuous spectral cascading processes. This model does yield an energy spectrum function which agrees with reported measurements quite well. However, scalar spectral measurements in turbulent flows with very large Reynolds number and Péclet number are needed for a more critical comparison with the deduced scalar spectrum function.

VII. SUMMARY

In the preceding sections we have proposed a continuous cascading process for turbulent energy and concentration transfer at large wavenumbers (the universal range). Based on this process, the energy spectrum function is deduced from (2.17) as

$$E(k) = \alpha\epsilon^{2/3}k^{-5/3} \exp\left(-\tfrac{3}{2}\alpha\nu\epsilon^{-1/3}k^{4/3}\right), \qquad k \gg k_0;$$

or, in simpler dimensionless form, as (2.18);

$$\tilde{E}(\tilde{k}) = \alpha\tilde{k}^{-5/3} \exp\left(-\tfrac{3}{2}\alpha\tilde{k}^{4/3}\right), \qquad \tilde{k} \gg \tilde{k}_0.$$

The resulting one-dimensional energy spectrum function $\varphi(k_1)$, (3.4), is in good agreement with observations obtained so far (see Figs. 5, 6, and 7). The deduced scalar spectrum function is, from (4.12),

$$F(k) = n\chi\epsilon^{-1/3}k^{-5/3} \exp\left(-\tfrac{3}{2}n\mathfrak{D}\epsilon^{-1/3}k^{4/3}\right), \qquad k \gg k_\theta,$$

which is independent of viscosity. In dimensionless form, from (4.14),

$$\hat{F}(\hat{k}) = \hat{n}\hat{k}^{-5/3} \exp\left(-\tfrac{3}{2}n\hat{k}^{4/3}\right), \qquad \hat{k} \gg \hat{k}_\theta.$$

The resulting one-dimensional scalar spectrum function $\psi(k_1)$, Eq. (5.4), is compared with measurements (see Fig. 10).

The concepts introduced in this analysis can further be applied to other convected passive quantities, such as weak magnetic field, in turbulent fluids.

ACKNOWLEDGMENT

The author is indebted to Professor John Laufer for reading the rough draft and for some helpful suggestions.